

## Investigation of Surface Interactions in Molecular Recognition of Phosphonate Imprinted Organosilicates and the Role of Water

Shalini Jayasundera,<sup>†,§</sup> Mazyar Zeinali,<sup>†</sup> Joel B. Miller,<sup>‡</sup> Luminita M. Velea,<sup>†</sup>  
Bruce P. Gaber,<sup>†</sup> and Michael A. Markowitz<sup>\*,†</sup>

Center for Bio/Molecular Science and Engineering, Code 6900, Naval Research Laboratory, Washington, D.C. 20375, and Chemistry Division, Code 6120, Naval Research Laboratory, Washington D.C. 20375

Received: June 21, 2006; In Final Form: August 3, 2006

Surface interactions in molecular recognition of phosphonate imprinted organosilicates and the role of water have been studied. NMR and calorimetry studies have shown the changing nature of the surface water structure on silicate surfaces due to template directed molecular imprinting. Results indicate the interaction of an organophosphonate compound with the functionalized silica surfaces to be through surrounding water molecules. However, with nonfunctionalized surfaces, additional higher energy interactions were possible. Further, our results support the possible templating effect of water during the imprint process.

Molecular imprinting creates solid surfaces with necessary shape factors and/or chemical functionality through reversible covalent and noncovalent interactions with (template) imprint molecules during synthesis to favor enhanced adsorption. While imprinting of organic polymers was first reported in 1972,<sup>1,2</sup> molecular imprinting of silica was reported as early as 1949 in which enhanced adsorption of dyes on the imprinted surface of silica gels was observed.<sup>3,4</sup> Recent publications have focused on imprinting of silica as robust catalysts or sorbents,<sup>5–10</sup> however the bulk of the molecular imprinting research has focused on imprinted organic polymers.<sup>11–12</sup> Noncovalent template imprinting of silica can be competently conceived, yet a mechanistic understanding and experimental success are more elusive.<sup>6,9,13–14</sup> In addition, surface water is expected to be a major player in the adsorption onto silica surfaces.<sup>15</sup> The role of the water molecules present on silicate surfaces has not been addressed with respect to imprinting. We previously reported significant enhancement in adsorption and selectivity of organophosphonates onto functionalized imprinted silica surfaces,<sup>16</sup> yet the mechanistic reasons for the enhancement and the effect of molecular imprinting were not self-evident.

### Introduction

Herein, we report the effect of template directed molecular imprinting for phosphonate compounds on silicate surfaces and the direct identification of the interactions on the imprinted surfaces. The influence of surface functionalization is also presented. Our study provides the required direct analysis by NMR and calorimetry data for the role of water on the adsorption of phosphonate compounds on template imprinted surfaces with strong implications toward the templating effect of water.

### Experimental Methods

**Materials.** Previously prepared silica surfaces,<sup>16</sup> Plain, Plain–PMP imprint, TMACPTMS, TMACPTMS–PMP imprint, PETMS, and PETMS–PMP imprint surfaces were used for this study. Pinacolyl methylphosphonate (PMP) was obtained from Aldrich Chemical Co.

**NMR Experiments.** The <sup>1</sup>H MAS NMR spectra were determined using Bruker DMX 400 and 500 spectrometers with MAS probes at 400.03 and 500.03 MHz, respectively. The number of data points in single-pulse experiments was 16 K. Samples were packed in 7 and 4 mm ZrO<sub>2</sub> rotors with tightly fitting Kel-F rotor caps to minimize the exchange of moisture with the outside. Magic angle spinning rates of up to 12.5 kHz were used. The proton chemical shifts were determined by external reference to tetrakis(trimethylsilyl)methane (TTMASH) at 0 ppm, and the liquid water peak is at 4.9 ppm. All peak positions, line widths, and relative peak intensities were determined from deconvolution of the <sup>1</sup>H MAS NMR spectra using a Lorentzian fit. Solid-state <sup>29</sup>Si and <sup>13</sup>C NMR experiments were performed at room temperature on a Bruker DMX 500 MHz at a resonance frequency of 99.36 and 125.77 MHz, respectively, with a 4.0 mm MAS probe. The samples were packed in 4 mm zirconia Bruker rotors fitted with Kel-F end caps for magic angle spinning at 5 kHz for <sup>29</sup>Si NMR and 10–12.5 kHz for <sup>13</sup>C NMR. A two-pulse phase modulation (TPPM) decoupling<sup>17</sup> was used for proton decoupling in the cross-polarization magic angle spinning (CP/MAS) and single-pulse (SP) experiments. A <sup>29</sup>Si CP contact time of 3 ms was used for all the samples with up to 6000 scans and 2–5 s recycle delays. Single-pulse MAS spectra with high power decoupling were recorded with 5 μs pulses and a recycle delay of 120 s. The <sup>29</sup>Si reference was set to external tetrakis(trimethylsilyl)silane at –9.9 (SiMe<sub>3</sub>) and –135.6 ppm (*T* = 297 K) with respect to TMS at 0 ppm. A <sup>13</sup>C CP contact time of 3 ms was used with up to 40 000 scans and 3 s delays. The <sup>13</sup>C reference was set to external tetrakis(trimethylsilyl)silane at 3.5 ppm with respect to TMS at 0 ppm. <sup>31</sup>P MAS NMR experiments were performed

\* To whom correspondence should be addressed. E-mail: Michael.Markowitz@nrl.navy.mil.

<sup>†</sup> Center for Bio/Molecular Science and Engineering, Naval Research Laboratory.

<sup>‡</sup> Chemistry Division, Naval Research Laboratory.

<sup>§</sup> Current address: Environmental Programs Group, Water Programs, Computer Sciences Corporation, Federal Sector, 6101 Stevenson Avenue, Alexandria, VA 22304.

on Bruker DMX 400 and 500 MHz instruments with 7.0 mm and 4.0 mm MAS probes. The  $^{31}\text{P}$  reference was set to external ammonium dihydrogenphosphate ( $(\text{NH}_4)_2\text{H}_2\text{PO}_4$ ) at 0.8 ppm or  $\text{Na}_2\text{HPO}_4$  at 6.6 ppm with respect to phosphoric acid at 0 ppm. All samples were packed in 7 and 4 mm  $\text{ZrO}_2$  rotors with tightly fitting Kel-F rotor caps.

**ITC and Adsorption Experiments.** ITC measurements of pinacolyl methylphosphonate–silica interactions were performed on a MicroCal VP-ITC titration microcalorimeter (MicroCal Inc., Northampton, MA). The modified silica powders, at ambient humidity or dried ( $2.2 \pm 0.2$  mg), and degassed anhydrous 2-propanol (a sufficient amount to completely fill the sample cell) were loaded into the ITC sample cell and allowed to equilibrate under stirring (580 rpm) for 1 h. The injection syringe contained a solution of PMP in degassed anhydrous 2-propanol (3.0, 1.0, or 0.6 mM). The titration was performed by repeated injections of 10  $\mu\text{L}$  volumes (25 total injections) at  $25 \pm 0.1$   $^\circ\text{C}$ . Heats of dilution were determined by performing similar titrations as above without the presence of silica powders (PMP dilution energy) or PMP (silica powder dilution energy). The calorimeter was calibrated with electrical pulses as outlined in the user's manual. The integral cumulative heats of adsorption ( $Q_{\text{cum}}^{\text{int}}$ ) were determined by the integration of the ITC peaks (ORIGIN software; MicroCal Software, Inc.) and the use of previously published adsorption isotherms.<sup>16</sup> Molar interaction energy ( $E_{\text{in}}^{\text{m}}$ ) was calculated by linear least-squares fit of  $Q_{\text{cum}}^{\text{int}}$  vs  $\Gamma$  (amount adsorbed).

Dried silica powders for ITC analysis were dried at 70  $^\circ\text{C}$  for up to 7 days followed by 12 h at 100  $^\circ\text{C}$  prior to ITC experiments. Drying of powders for adsorption experiments was performed by placing powders in eppendorf microcentrifuge tubes and placing in an oven at 70  $^\circ\text{C}$  for up to 7 days to partially remove surface bound water. This method was used to remove a large portion of the physically bound water yet allow for some surface water to remain. Thermogravimetric analysis confirmed the removal of at least 60% of surface water, yet also showed that, to remove surface bound water completely, a temperature greater than 140  $^\circ\text{C}$  had to be used. Solid-state NMR confirmed that the drying method removed surface water and was not destructive to the surface structure. All dried silicates for ITC analysis were stored under vacuum and Drierite to minimize reabsorption of surface moisture.

Adsorption experiments were performed by the addition of 1 mL of 3 mM PMP in anhydrous 2-propanol to a microcentrifuge tube containing 15 mg of the dried silica particles or 3mM PMP in DI to tubes containing nondried silica. The mixture was shaken on a vortex shaker for 30 min then centrifuged for the separation of particles and solution. The supernatant was analyzed for PMP as outlined previously.<sup>16</sup>

## Results and Discussion

In a detailed study, a combination of  $^1\text{H}$ ,  $^{29}\text{Si}$ ,  $^{31}\text{P}$ , and  $^{13}\text{C}$  solid-state NMR was used to investigate the changes in the adsorbed water layer characteristics, the active surface sites, the organic functional groups, and adsorbed complexes. The thermodynamic parameters directly measured through isothermal titration calorimetry provided the relevant energy changes during molecular interactions. The effect of molecular imprinting, with pinacolyl methylphosphonate (PMP), on silica surfaces prepared by polymerizing tetraethoxysilane (TEOS) (referred to as Plain) and copolymerizing TEOS with the functionalized silanes *N*-trimethoxysilylpropyl-*N,N,N*-trimethylammonium chloride (referred to as TMACPTMS) and 2-(trimethoxysilyl)ethylpyridine

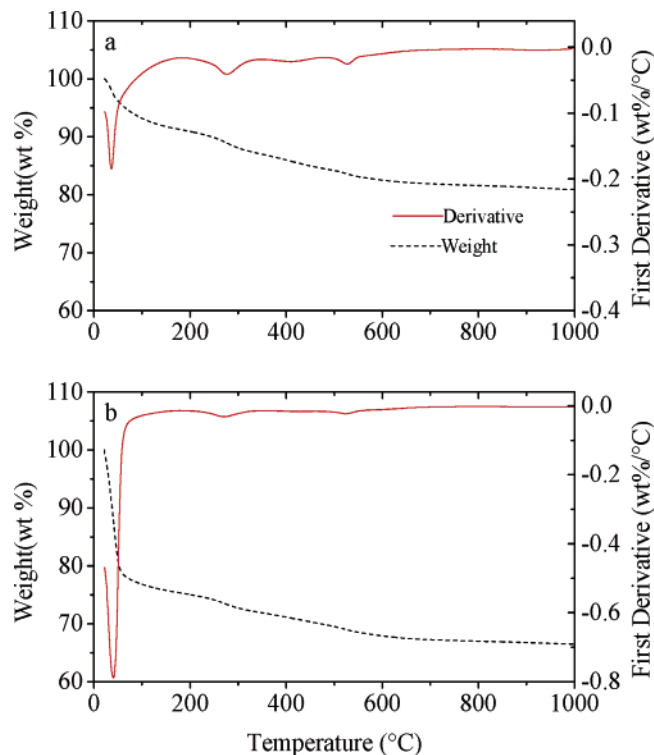


**Figure 1.** TGA (weight vs  $T$ ) and first derivative curves of TMACPTMS functionalized silica for (a) nonimprinted and (b) imprinted surfaces. Temperature program from ambient to 1000  $^\circ\text{C}$  at 10  $^\circ\text{C}$  per min.

(referred to as PETMS) were evaluated by observing the changes to the silanol ( $\equiv\text{SiOH}$ ) groups and adsorbed water in the overall structure of the silica particles.

The surface functionality of the silica surfaces prepared with and without the functionalized silanes was analyzed using  $^{29}\text{Si}$  MAS NMR. The C–Si bonds in the functionalized silicates showed no cleavage, and the atomic structure of the silicon atoms did not change due to imprinting. The physisorbed water was studied using thermogravimetric analysis (TGA) and  $^1\text{H}$  MAS NMR. The TGA results showed an increase in the physically adsorbed water content in the imprinted vs the nonimprinted surfaces with the largest increase ( $\approx 5$  wt %) in the TMACPTMS functionalized imprinted silica. However, the amount of physically bound water in silica surfaces is also dependent on factors such as humidity in the environment during sample preparation, and thus, its quantitative correlation with factors such as degree or type of functionalization is difficult at best. A change in the removal rate of the physically adsorbed water, as evident in the first derivative of TGA plots (Figure 1), was also observed with the imprinted surfaces showing a greater removal rate with a sharper/less broad peak in zone 1 (i.e., 140–160  $^\circ\text{C}$  temperature region). Imprinted TMACPTMS showed the largest rate increase where the rate more than doubled from 1 to 2.5 wt %/min. This suggests a change in the nature of the physically adsorbed water with weaker water–surface interactions due to imprinting. Due to the weaker interactions between the water molecules and the silicate surface in imprinted TMACPTMS, the water protons were easily available for deuterium exchange and removal through magic angle spinning in an unsealed rotor when monitored through  $^1\text{H}$  MAS NMR.<sup>18</sup>

Imprinting with PMP also resulted in more narrow and symmetrical line shapes of the  $^1\text{H}$  MAS NMR peaks of the water and the hydrogen bonded silanols compared with those in the nonimprinted surfaces. A general upfield shift of the proton

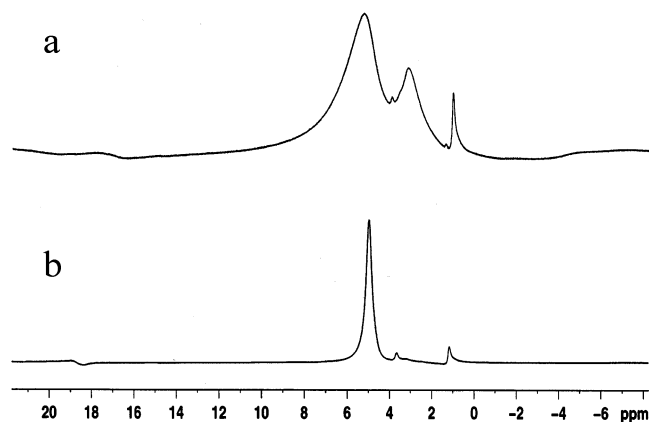


**Figure 2.**  $^1\text{H}$  MAS NMR spectra of (a) nonimprinted and (b) imprinted TMACPTMS surfaces.

frequencies was also observed upon imprinting. The most significant difference in the water frequencies was observed in the TMACPTMS imprinted surface, compared to its nonimprinted surface (Figure 2). The broad peak at 5.39 ppm in the nonimprinted TMACPTMS surface shows the presence of bound water with variable degrees of condensation and lower mobility on the silicate structure. Silanols hydrogen bonded to water molecules, involved in chemical exchange, may also be contained within this broad peak.<sup>19</sup> A more narrow water peak width was observed in the imprinted surface compared with the nonimprinted surface (0.85 ppm at 4.96 ppm compared with 2.08 ppm at 5.39 ppm) indicating a change in the nature of the physically bound water. The chemical shifts of the physically bound water peaks in imprinted surfaces were closer to that of clustered liquid water<sup>20</sup> (4.9 ppm). These observations clearly show changes to the mode of water interaction during molecular imprinting with PMP in that the nature of the physically bound water in the imprinted surfaces was displaced to more “water-like” clusters and more “free” in nature. In addition, we found that acidification of imprinted TMACPTMS resulted in the “free” water peak at 4.96 ppm becoming more strongly bound similar to that of the nonimprinted TMACPTMS.

Changes to the physically bound surface water can have significant effects on PMP–surface interactions. Peak integration of a series of liquid  $^1\text{H}$  NMR spectra of PMP in anhydrous propanol, open to the atmosphere, showed an increasing number

of water molecules interacting at and near the –OH proton site of PMP indicating that supra assemblies of water molecules surround PMP (data not shown) creating a water shell. This later finding in addition to the changes in the interaction modes of the surface water resulting from molecular imprinting suggests that the assembly of water molecules surrounding PMP during synthesis may play a role in the template imprinting process for PMP. Thus, the solvation shell of PMP may form an imprint cavity/shape factor on the silica surface. Recently, Henry et al.<sup>21</sup> opened a discussion for the possibility of the templating effect of water clusters on nanoporous structures through energy minimization calculations and X-ray powder diffraction studies of the organic framework of MIL 74 ( $\text{Zn}_6\text{Al}_{12}\text{P}_{24}\text{O}_{96} \cdot [\text{N}(\text{CH}_2\text{CH}_2\text{NH}_3)_3]_8 \cdot (\text{H}_2\text{O})_{34}$ ). Our study provides strong evidence for the role of water in the imprinting process.

The adsorption of PMP onto the silica powders was highly dependent on the presence of physically bound surface water. Adsorption experiments with partially dried silica powders confirmed the significance of surface water in PMP adsorption. There was an  $\sim 70\%$  reduction in PMP adsorption ( $\Gamma$ ) when  $\sim 60\%$  of the surface bound water was removed. Virtually no PMP adsorbed onto PMP imprinted TMACPTMS when experiments were performed in DI water rather than in anhydrous 2-propanol, further confirming the PMP preference for water. Figure 3 shows the  $^1\text{H}$  NMR spectra of the PMP sorbed functionalized imprinted surfaces of TMACPTMS and PETMS. A significant signal broadening, lowering of intensity, and a downfield shift of the physically bound water peak (peak at  $\sim 4.9$  ppm marked with an arrow) were observed for PMP adsorption onto imprinted silicate surfaces. The peak broadening and lowering in intensity is due to the reduced mobility of the now interacting water molecules either with the imprinted surface or PMP. A significantly smaller effect was observed in the more strongly bound water peaks of the nonimprinted surfaces when PMP was adsorbed.<sup>22</sup> Water molecules which are strongly complexed with the surface do not contribute to  $\Delta G$  (change in Gibbs free energy) of adsorption<sup>15</sup> and will not be involved in the formation of PMP surface complexes. These results specify the relative importance of the surface bound water in the adsorption of PMP.

Figures 4 and 5 illustrate the cumulative heats of interaction as a function of surface loading ( $\theta = \Gamma/\Gamma_{\text{max}}$ ) and amount adsorbed ( $\Gamma$ ).<sup>23</sup> For Plain silica, the titrations revealed constant

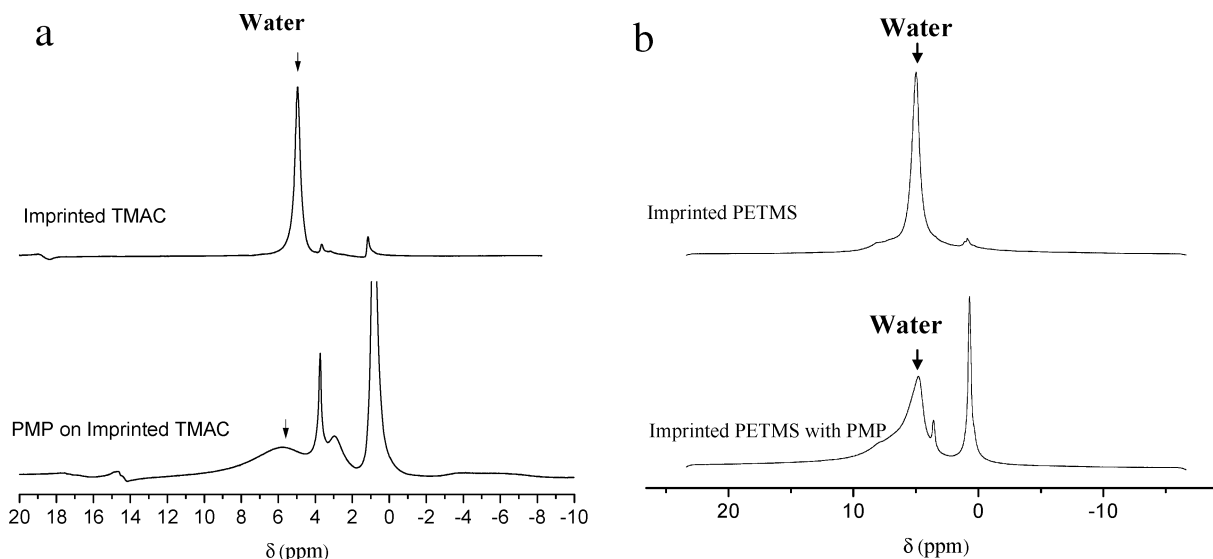


**Figure 3.**  $^1\text{H}$  MAS NMR spectra showing changes in the water protons of functionalized silicates due to PMP adsorption: (a) imprinted TMACPTMS and (b) imprinted PETMS surfaces. The water proton frequencies are shown with an arrow.

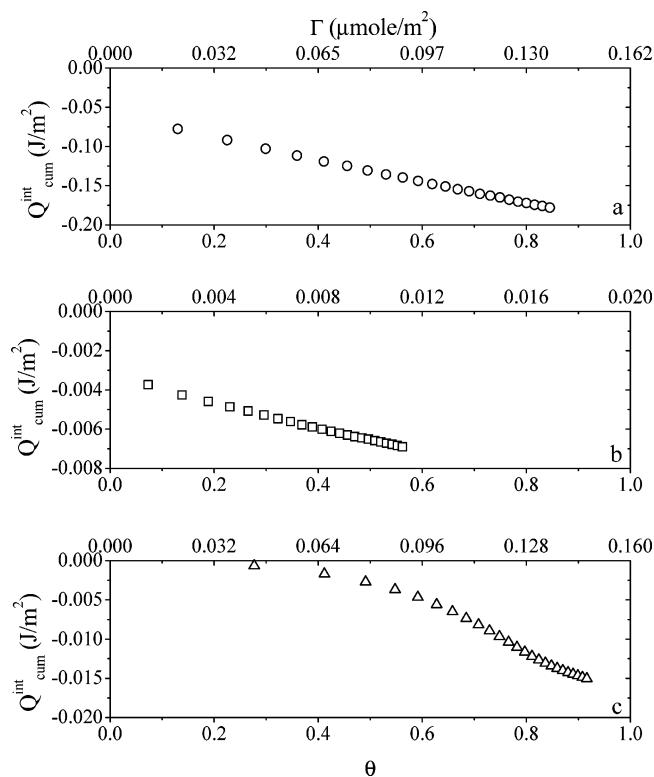
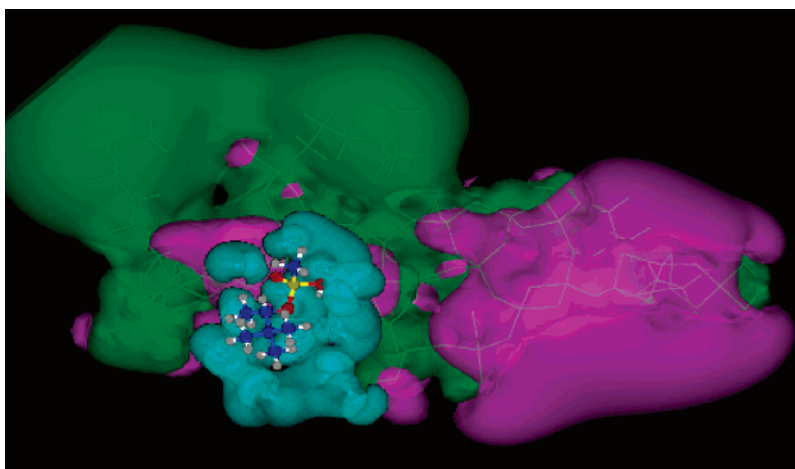


**Figure 4.** PMP interaction energy with nonimprinted (a) Plain, (b) PETMS, and (c) TMACPTMS silica.

heats of interaction for both nonimprinted and imprinted surfaces as shown in the linearity of the heats. However, for the functionalized surfaces, the interaction heats became less linear. Table 1 lists the molar interaction energies ( $E_{in}^m$ ) of PMP with the surfaces including the linear correlation coefficients. Adsorption enthalpy and/or interaction energies are highly sensitive to changes in modes of interaction, thus the nonlinearity of the heats for the functionalized surfaces suggests changes in and/or additional interactions occurring as a function of surface loading.  $^{13}\text{C}$  CPMAS NMR studies revealed that some of the positively charged amino end groups of TMACPTMS and pyridine end groups of PETMS in the functionalized silicas show electrostatic (polar) interactions and hydrogen bonding to the silanols on the imprinted surfaces, respectively.<sup>24</sup> Dipolar

**SCHEME 1. PMP Interactions on an Imprinted TMACPTMS Surface Occurring through Surface Water Molecules Surrounding PMP<sup>a</sup>**



<sup>a</sup> For clarity purposes, those water molecules on the remaining surface are not shown.

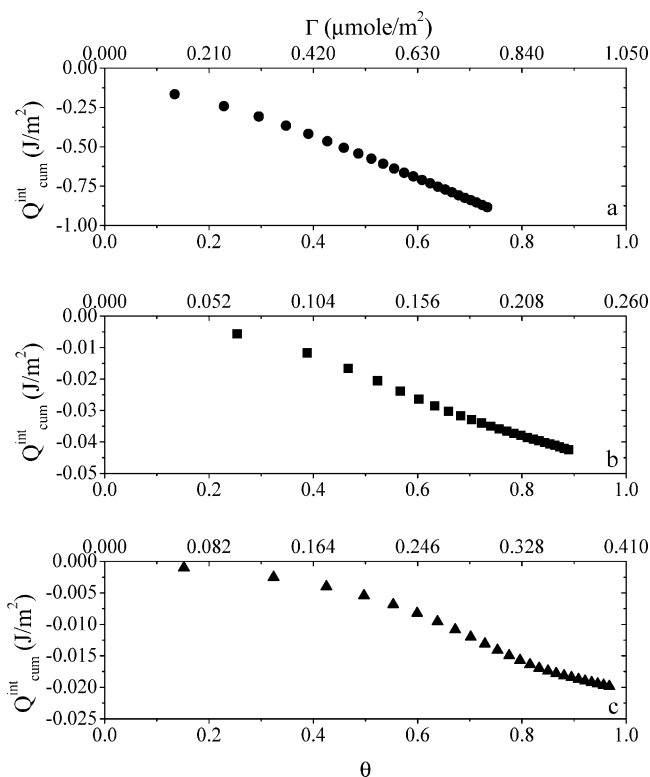


**Figure 5.** PMP interaction energy with PMP imprinted (a) Plain, (b) PETMS, and (c) TMACPTMS silica.

**TABLE 1: PMP Interaction Energy with Silica Surfaces**

silica	$E_{in}^m$ (kJ/mol)	$R^2$
Plain	860	0.999
Plain imprinted	1200	0.995
PETMS	320	0.997
PETMS imprinted	230	0.995
TMACPTMS	170	0.977
TMACPTMS imprinted	70	0.967

dephasing experiments showed only a partial decay of the  $^{13}\text{C}$  spins in the organic functional groups indicating that some of the organic functional group backbones were not strongly bound/restricted and were free to move while some others folder over



to form surface interactions.<sup>25</sup> These different functional group environments became one and gave way to PMP–water–surface interactions when PMP was adsorbed. This behavior which was mostly observed in the imprinted surfaces may partially explain the nonlinearity of the heats of adsorption in the functionalized surfaces.

Furthermore, although linear heats were observed for Plain (suggesting a single dominant interaction mechanism in terms of the energy), the interaction energies were almost 3 times greater (860 vs 320 and 170 kJ/mol) in comparison to the functionalized nonimprinted surfaces and more than 5 times greater (1200 vs 230 and 70 kJ/mol) for the imprinted Plain surface. These high energies in the Plain surfaces are consistent with covalent type interactions occurring at the surface.<sup>26</sup> <sup>31</sup>P CPMA S NMR experiments show a strongly bound secondary peak for the PMP sorbed Plain surfaces suggesting a phosphorylation type interaction initiated by the stronger Lewis acidity of the Plain surface, which may also be occurring.<sup>27</sup>

Only noncovalent interactions were observed between PMP and the functionalized surfaces<sup>28</sup> and are consistent with the lower molar interaction energies observed. Further, the <sup>29</sup>Si MAS NMR signal for Si–OH, where possible covalent interactions can occur at the surface, slightly reduced in intensity when PMP was sorbed further pointing toward some reversible covalent interactions occurring between PMP and the Plain surface. However, further research is needed to confirm the secondary covalent interaction.

In conclusion, our study shows strong evidence for the changing nature of the surface water structure on silicate surfaces due to imprinting with PMP revealing the role of the surrounding water assembly of PMP in the imprinting process. The rearrangement of the nature of water molecules due to imprinting resulted in increased adsorption on imprinted surfaces likely due to the more “free” water clusters being available to form water shells around PMP allowing for the formation of more favorable interactions with the surface (Scheme 1). In the absence of surface–water–PMP interactions to a specific surface, sites created as a result of molecular imprinting and/or surface functionalization are most likely ancillary or negligible.

**Acknowledgment.** The authors thank the Office of Naval Research for providing funding for this work. S.J., M.Z., and L.V. are National Research Council Postdoctoral Fellows. We thank W. F. Schmidt for his support during this research. The views expressed here are those of the authors and do not

necessarily represent those of the U.S. Navy, the U.S. Department of Defense, or the U.S. Government. S.J. and M.Z. have made equal contributions to this work.

**Supporting Information Available:** Detailed drying procedures, supporting ITC figures and tables, supporting NMR figures, and interpretations. This material is available free of charge via the Internet at <http://pubs.acs.org>.

## References and Notes

- (1) Wulff, G.; Sarhan, A. *Angew. Chem., Int. Ed. Engl.* **1972**, *11*, 341.
- (2) Wulf, G.; Sarhan, A.; Zabrocki, K. *Tetrahedron Lett.* **1973**, 4329–4332.
- (3) Dickey, F. H. *Proc. Natl. Acad. Sci.* **1949**, *35*, 227–229.
- (4) Dickey, F. H. *J. Phys. Chem.* **1955**, *59*, 695–707.
- (5) Wulff, G.; Heide, B.; Helfmeier, G. *J. Am. Chem. Soc.* **1986**, *108*, 1089–1091.
- (6) Heilmann, J.; Maier, W. F. *Angew. Chem., Int. Ed. Engl.* **1994**, *33*, 471–473.
- (7) Dai, S.; Burleigh, M. C.; Shin, Y.; Morrow, C. C.; Barnes, C. E.; Xue, Z. *Angew. Chem., Int. Ed.* **1999**, *38*, 1235–1239.
- (8) Markowitz, M. A.; Kust, P. R.; Deng, G.; Schoen, P. E.; Dordick, J. S.; Clark, D. S.; Gaber, B. P. *Langmuir* **2000**, *16*, 1759–1765.
- (9) Katz, A.; Davis, M. E. *Nature* **2000**, *403*, 286–289.
- (10) Markowitz, M. A.; Kust, P. R.; Klaehn, J.; Deng, G.; Gaber, B. P. *Anal. Chim. Acta* **2001**, *435*, 177–185.
- (11) Wulff, G. *Angew. Chem., Int. Ed. Engl.* **1995**, *34*, 1812–1832.
- (12) Whitcombe, M. J.; Vulfson, E. N. *Adv. Mater.* **2001**, *13*, 467–479.
- (13) Ahmad, W. R.; Davis, M. E. *Catal. Lett.* **1996**, *40*, 109–114.
- (14) Maier, W. F.; Mustapha, B. *Catal. Lett.* **1997**, *46*, 137–140.
- (15) Turov, V. V.; Gun'ko, V. M.; Zarko, V. I.; Bogatyr'ov, V. M.; Dudnik, V. V.; Chuiko, A. A. *Langmuir* **1996**, *12*, 3503–3510.
- (16) Markowitz, M. A.; Deng, G.; Gaber, B. P. *Langmuir* **2000**, *16*, 6148–6155.
- (17) Bennett, A. E.; Rienstra, C. M.; Auger, M.; Lakshmi, K. V.; Griffin, R. G. *J. Chem. Phys.* **1995**, *103*, 6951–6956.
- (18) See Supporting Information Figure S1.
- (19) Grunberg, B.; Emmeler, T.; Gedat, E.; Shendeerovich, I.; Findenegg, G. H.; Limbach, H.; Buntkowsky, G. *Chem.–Eur. J.* **2004**, *10*, 5689–5696.
- (20) Turov, V. V.; Gun'ko, V. M.; Bogatyr'ov, V. M.; Zarko, V. I.; Gorbik, S. P.; Pakhlov, E. M.; Leboda, R.; Shulga, O. V.; Chuiko, A. A. *J. Colloid Interface Sci.* **2005**, *283*, 329–343.
- (21) Henry, M.; Taulelle, F.; Loiseau, T.; Beitone, L.; Ferey, G. *Chem.–Eur. J.* **2004**, *10*, 1366–1372.
- (22) See Supporting Information Figure S2.
- (23) See Supporting Information Figures S3 and S4 for representative ITC thermograms.
- (24) See Supporting Information: Functional Group Surface Interactions and Figures S5 and S6.
- (25) See Supporting Information Scheme S1.
- (26) Lukes, I.; Borbaruah, M.; Quin, L. D. *J. Am. Chem. Soc.* **1994**, *116*, 1737–1741.
- (27) See Supporting Information Figure S7 and Scheme S2.
- (28) See Supporting Information Figure S8.